

# Incorporation rate measurements of $^{10}\text{Be}$ , $^{230}\text{Th}$ , $^{231}\text{Pa}$ , and $^{239,240}\text{Pu}$ radionuclides in manganese crust in the Pacific Ocean: A search for extraterrestrial material

メタデータ	言語: eng 出版者: 公開日: 2017-10-03 キーワード (Ja): キーワード (En): 作成者: 横山, 明彦, 中西, 孝 メールアドレス: 所属:
URL	<a href="https://doi.org/10.24517/00010228">https://doi.org/10.24517/00010228</a>

This work is licensed under a Creative Commons Attribution-NonCommercial-ShareAlike 3.0 International License.



# **Incorporation Rate Measurements of $^{10}\text{Be}$ , $^{230}\text{Th}$ , $^{231}\text{Pa}$ , and $^{239, 240}\text{Pu}$ Radionuclides in Manganese Crust in the Pacific Ocean in Search for Extraterrestrial Material**

NORIKAZU KINOSHITA<sup>1\*</sup>, YUKO SATO<sup>1</sup>, TAKEYASU YAMAGATA<sup>2</sup>, HISAO NAGAI<sup>3</sup>,  
AKIHIKO YOKOYAMA<sup>1</sup> and TAKASHI NAKANISHI<sup>1</sup>

<sup>1</sup>*Graduate School of Natural Science and Technology, Kanazawa University, Kakuma, Kanazawa, Ishikawa 920–1192, Japan*

<sup>2</sup>*Graduate School of Integrated Basic Sciences, Nihon University, 3–25–40 Sakura-Josui, Setagaya, Tokyo 156–8550, Japan*

<sup>3</sup>*College of Humanities and Sciences, Nihon University, 3–25–40 Sakura-Josui, Setagaya, Tokyo 156–8550, Japan*

\*Corresponding author. E-mail: [norikazu@post.kek.jp](mailto:norikazu@post.kek.jp)

Present address: Radiation Science Center, High Energy Accelerator Research Organization (KEK), 1–1 Oho, Tsukuba, Ibaraki 305–0801, Japan

## **Abstract**

In order to estimate the deposition rate of extraterrestrial material onto a manganese crust in a project to search for supernova debris, we analyzed the contents of  $^{10}\text{Be}$ ,  $^{230}\text{Th}$ ,  $^{231}\text{Pa}$ , and  $^{239,240}\text{Pu}$  in a sample of manganese crust collected from the North Pacific Ocean. On the basis of the depth profile of  $^{10}\text{Be}$ , the growth rate of the manganese crust was determined to be  $2.3 \text{ mm Myr}^{-1}$ . The uptake rates of  $^{10}\text{Be}$ ,  $^{230}\text{Th}$ , and  $^{231}\text{Pa}$  onto the manganese crust were estimated to be 0.22–0.44%, 0.11–0.73%, and 1.4–4.5%, respectively, as compared to the deposition rates onto the deep-sea sediments near the sampling station and that for  $^{239,240}\text{Pu}$  was 0.14% as compared to the total inventory of seawater and sediment column. Assuming the sinking particles to be 0.11–4.5% of the uptake rates, the deposition rate of extraterrestrial material onto the manganese crust was estimated to be  $2\text{--}800 \mu\text{g cm}^{-2} \text{ Myr}^{-1}$  according to the uptake of  $^{10}\text{Be}$  onto the manganese crust. Further, our estimate is similar to the value of  $9\text{--}90 \mu\text{g cm}^{-2} \text{ Myr}^{-1}$  obtained using the integrated global production rate of  $^{10}\text{Be}$  and the deposition rate of  $^{10}\text{Be}$  onto the manganese crust.

## **Keywords:**

- Manganese crust,
- Natural and artificial radionuclides
- Depth profile,
- Deposition rate,
- Uptake rate

## 1. Introduction

Manganese encrustation present on the ocean floor is a mysterious material that grows very slowly and consists of manganese oxide and iron oxide as the main components. It has been considered that a manganese encrustation receives trace elements from seawater during the grow process. In addition, it was reported that extraterrestrial debris might be taken into manganese encrustations as evidenced by its  $^3\text{He}/^4\text{He}$  isotopic ratio (Sano et al., 1985; Basu et al., 2006). Recently, the so-called extinct nuclides, such as  $^{60}\text{Fe}$  ( $T_{1/2} = 1.51 \times 10^6$  yr) and  $^{244}\text{Pu}$  ( $T_{1/2} = 8.08 \times 10^7$  yr) that are not expected in the solar system because their half-lives are sufficiently shorter than the age of the solar system, were found in a manganese encrustation by Knie et al. (1999), Wallner et al. (2000), Knie et al. (2004), and Wallner et al. (2004). Knie et al. (2004) found a highly significant increase in the  $^{60}\text{Fe}$  concentration around 2.8 Myr ago in a dated deep-sea manganese crust by using an accelerator mass spectrometer (AMS). Wallner et al. (2004) attempted to detect  $^{244}\text{Pu}$  in 120 g of a fallout-free part of a deep-sea manganese crust using an AMS. One single  $^{244}\text{Pu}$  event was observed, and this count corresponds to the terrestrial inputs at around  $3 \times 10^4$  atoms  $\text{cm}^{-2}$  during the period from 1 to 14 Myr. However, a much larger sample is required to improve the statistics and reliability.

Deep-sea manganese crusts and nodules appear to be one of the strongest candidates for searching supernova debris that have been deposited on the earth's surface, because these samples can be obtained in large quantities. The surface layer of the manganese crusts and nodules contaminated with anthropogenic radionuclides can be easily discernable by establishing geochronology and a negligible mobility of radionuclides in the ferromanganese encrustation.

Naturally occurring radionuclides such as  $^{10}\text{Be}$ ,  $^{230}\text{Th}$ , and  $^{231}\text{Pa}$  are often used for estimating the growth rates of manganese encrustations in the sea and for other geochemical studies. The  $^{10}\text{Be}$  nuclides are produced from the nuclear spallation of atoms by cosmic rays in the upper atmosphere, and  $^{230}\text{Th}$  and  $^{231}\text{Pa}$  are the daughters of  $^{238}\text{U}$  and  $^{235}\text{U}$ , respectively.

$^{244}\text{Pu}$  nuclides and other Pu isotopes have been produced from natural supernova explosions and hence they also have an interstellar origin and anthropogenic means. Materials on the entire surface of the earth have been subjected to anthropogenic radionuclide contamination largely produced from the atmospheric thermo nuclear bomb tests conducted from 1945 to 1980 (Buesseler, 1997; UNSCEAR, 2000; Aarkrog, 2003). Theoretically, Pu isotopes may be used for estimating the growth rates for slow-growing manganese encrustations in the sea; however, no substantial work has been carried out. The residence times of  $^{10}\text{Be}$ ,  $^{230}\text{Th}$ ,  $^{231}\text{Pa}$ , and  $^{239,240}\text{Pu}$  in an ocean water column are estimated to be ~1000 yr, 10–40 yr, ~100 yr, and ~400 yr, respectively (Lao et al., 1993; Livingston and Anderson, 1983); these values suggest that their affinities with suspended and sinking particulate matter are not the same. Additionally, the deposition rates of nuclides are important for obtaining information about the concentration factor in searching for extinct nuclides.

In the present work, we determined the depth distributions of  $^{10}\text{Be}$ ,  $^{230}\text{Th}$ ,  $^{231}\text{Pa}$ , and  $^{239,240}\text{Pu}$ .  $^{239,240}\text{Pu}$  in the manganese crust was utilized as a proxy for  $^{244}\text{Pu}$  to estimate its concentration factor in the manganese encrustation with respect to those of ambient seawater and bottom sediments and later to use it for the flux of  $^{244}\text{Pu}$  having its origins in an interstellar medium. The deposition rates of natural and anthropogenic nuclides onto the manganese crust were also estimated and the possible deposition rate of extraterrestrial material onto the crust was discussed.

## **2. Experimental**

### *2.1 Sample*

A piece of manganese crust with a surface area of ca. 420 cm<sup>2</sup> and thickness of ca. 4.5 cm was obtained from the cruise of R. V. Hakurei-Marun No. 2, Japan Oil, Gas and Metals National Corporation, as a research project investigating cobalt-rich-crust ores. The sample

was dredged in 1994 on a sea mount at a water depth of 1551 m located between Johnston Island (16° N, 169° W) and Wake Island (19° N, 166° E). The crust was sliced into 5-mm-thick pieces; each piece was used in the present analysis.

## 2.2 Isolation and measurement of Th and Pu

Thorium and Pu isotopes were purified using a conventional ion-exchange technique. A known amount of the portion of the sliced manganese crust was dissolved in HCl digestion and a few drops of H<sub>2</sub>O<sub>2</sub>, immediately after adding <sup>242</sup>Pu and <sup>234</sup>Th as yield tracers. A <sup>234</sup>Th spike solution was obtained from uranium with a natural isotopic abundance and purified using a cation exchange column. After the removal of insoluble components such as silica by centrifugation, Th and Pu ions were coprecipitated with ammonia water. The precipitate was dissolved in 8 M HNO<sub>3</sub>, and the solution was reduced with H<sub>2</sub>O<sub>2</sub> to convert the oxidation state of Pu into Pu(IV). Then, the solution was allowed to pass through an anion exchange column (Dowex 1X8, 100–200 mesh) to elute the Th ions with 8 M HCl and then Pu ions with 8 M HCl – 0.1 M HI solution. After drying up the Pu effluent, the Pu species were dissolved in 0.2 M HCl with hydroxylamine hydrochloride; then, an Ag plate was soaked in the solution to remove Po in order to reduce the <sup>210</sup>Po atoms (Schultz et al., 2006), which disturb the measurement of the low-level activities of <sup>239</sup>, <sup>240</sup>Pu for alpha spectrometry. Purified Th and Pu were separately dissolved in an ammonium sulfate solution, followed by electrodeposition on a stainless steel disk. The recovery yield of Th was determined using a GM counter referring to a natural uranium standard covered with an Al foil with a thickness of 25 mg cm<sup>-2</sup> to cut the low-energy beta rays from <sup>234</sup>Th. The alpha activities of <sup>230</sup>Th and <sup>239</sup>, <sup>240</sup>Pu isotopes were measured using a silicon surface barrier detector with a counting efficiency of 25%. As an example, the alpha spectra of Pu samples are shown in Fig. 1. The <sup>239</sup>, <sup>240</sup>Pu content below 0.5 cm is extremely low. If the chemical purification is insufficient, tailing from the energetic alpha rays of radioactive contaminants overlaps alpha-ray peak of

$^{239, 240}\text{Pu}$ . Thus, a careful chemical separation is required for the determination of ultra low-level radioactivity of  $^{239, 240}\text{Pu}$ .

### *2.3 Isolation and measurement of Pa*

Protactinium isotopes were purified using a conventional solvent extraction and ion-exchange technique. A known amount of another portion of the sliced manganese crust was dissolved as described earlier. After the solution was spiked by  $^{233}\text{Pa}$  purified from  $^{237}\text{Np}$  through solvent extraction using diisobutylketone (DIBK) as an extractant, the Pa ions were coprecipitated with ammonia water. The precipitate was dissolved in 8 M HCl and the Pa ions were extracted to DIBK. After the ions were recovered by 3 M HCl, the Pa solution was evaporated up to dryness and converted to 8 M  $\text{HNO}_3$  solution. Then, the solution was allowed to pass through an anion exchange column (Dowex 1X8, 100–200 mesh) to elute the Pa ions with 8 M HCl – 0.1 M HF solution after the removal of Th ions using 8 M HCl. The Pa ions were electrodeposited on a stainless steel disk; then, the  $^{231}\text{Pa}$  activity was assayed in the same manner as that for the Th isotope described earlier.

### *2.4 Isolation and measurement of Be*

Beryllium isotopes were purified according to the method proposed by Shibata et al. (1998) with a little modification. A known amount of another portion of the sliced manganese crust was dissolved as described earlier. After the addition of 5 mg of a Be carrier and ethylenediaminetetraacetate (EDTA) as the masking reagent, the solution was adjusted to a pH of approximately 6 by using ammonia water. The Be ions were extracted to acetylacetone dissolved in a  $\text{CCl}_4$  solution; then, the ions in the organic phase were recovered to the aqueous phase with 8 M HCl. The solution was allowed to pass through an anion exchange column (Dowex 1X8, 100–200 mesh). Subsequently, the Be solution adjusted to 1 M HCl was allowed to pass through a cation exchange column (Dowex 50WX8, 200–400 mesh). The Be

in the solution was precipitated by using ammonia water (TAMA-PURE AA) and the precipitate was washed with Milli-Q water to remove the  $^{10}\text{B}$  atoms that disturb the following measurement. The  $^{10}\text{Be}$  measurements by an AMS were made in the Micro Analysis Laboratory, Tandem Accelerator, Research Center for Nuclear Science and Technology, University of Tokyo (MALT) (Matsuzaki et al., 2000).

### 3. Results and Discussion

#### 3.1 Profiles of radionuclides and growth rate estimation

The activity and atomic concentrations of the nuclides were converted to inventory per unit area ( $\text{Bq cm}^{-2}$  or  $\text{atoms cm}^{-2}$ ) for investigating the incorporation rate using the total surface area, the total weight of each piece, and the weight of the manganese crust used for the experiment. The depth profiles of  $^{10}\text{Be}$ ,  $^{230}\text{Th}$ ,  $^{231}\text{Pa}$ , and  $^{239,240}\text{Pu}$  in the manganese crust are shown in Figs. 2–5, respectively. The depth profile of  $^{238}\text{U}$  in a small portion of the sample measured using a SEIKO SPQ-9000 ICP-MS is shown in Fig. 6 in order to indicate disequilibrium/equilibrium. The activity ratios of  $^{230}\text{Th}/^{238}\text{U}$  and  $^{231}\text{Pa}/^{235}\text{U}$  are also shown in Fig. 3 and Fig. 4, respectively. The radioactivity of  $^{235}\text{U}$  used for the calculation of the activity ratio of  $^{231}\text{Pa}/^{235}\text{U}$  was estimated from the radioactivity of  $^{238}\text{U}$  using their isotopic abundances and half-lives, assuming the activity ratio of  $^{235}\text{U}/^{238}\text{U}$  to be constant everywhere. In the measurement involving the Pu isotopes, the count rates of  $^{239,240}\text{Pu}$  below 0.5 cm are insignificant as compared to the detection limit  $D_L$  estimated using the following equation which is also indicated by the broken line.

$$D_L = \frac{4}{t} \left( 1 + \sqrt{1 + 2Bt} \right), \quad (1)$$

where  $t$  is the measuring time for the Pu sample and  $B$  is the background count rate of the  $^{239,240}\text{Pu}$  region.  $^{239,240}\text{Pu}$  and the disequilibrium of  $^{230}\text{Th}$  and  $^{231}\text{Pa}$  were observed in the surface

of the manganese crust. The growth rate of the sample was determined to be  $2.3 \text{ mm Myr}^{-1}$  from the  $^{10}\text{Be}$  measurement under the assumptions that the diffusion of the Be atom is negligible and the supply rate from outside is constant.

### 3.2 Incorporation of radionuclides onto manganese crust

The unsupported activities of  $^{230}\text{Th}$  and  $^{231}\text{Pa}$  per unit area of the manganese crust, expressed as  $^{230}\text{Th}_{\text{exc}}$  and  $^{231}\text{Pa}_{\text{exc}}$ , for 0–0.5 cm were roughly estimated to be  $0.10 \text{ Bq cm}^{-2}$  and  $1.2 \times 10^{-2} \text{ Bq cm}^{-2}$ , respectively, simply by subtracting the average value at 0.5–4.5 cm from the activity observed at 0–0.5 cm, assuming that these nuclides below 0.5 cm are in radioactive equilibrium with the relevant parent nuclides. In addition, the  $^{10}\text{Be}$  content is calculated to be  $9.5 \times 10^9 \text{ atoms cm}^{-2}$  by the integration of the activity concentration from the surface to a depth of 4.5 cm in the crust.  $^{230}\text{Th}_{\text{exc}}$ ,  $^{231}\text{Pa}_{\text{exc}}$ , and  $^{10}\text{Be}$  contents per unit area of the manganese crust are expressed as follows in the unit of  $\text{Bq cm}^{-2}$  or  $\text{atoms cm}^{-2}$ .

$$S = \int_0^t A_0 e^{-\lambda t} dt, \quad (2)$$

where  $A_0$  is the deposition rate ( $\text{Bq cm}^{-2} \text{ yr}^{-1}$  or  $\text{atoms cm}^{-2} \text{ yr}^{-1}$ ),  $\lambda$  is the decay constant of a nuclide ( $\text{yr}^{-1}$ ), and  $t$  is the date of the layer of the manganese crust determined from the  $^{10}\text{Be}$  measurement (yr). From Eq. (2), the following expression was derived:

$$S = \frac{A_0}{\lambda} (1 - e^{-\lambda t}). \quad (3)$$

By using this equation, the deposition rate onto the manganese crust  $A_0$  was determined to be  $9.2 \times 10^{-7} \text{ Bq cm}^{-2} \text{ yr}^{-1}$  for  $^{230}\text{Th}$ ,  $2.5 \times 10^{-7} \text{ Bq cm}^{-2} \text{ yr}^{-1}$  for  $^{231}\text{Pa}$ , and  $4.4 \times 10^3 \text{ atoms cm}^{-2} \text{ yr}^{-1}$  for  $^{10}\text{Be}$ .

In the discussion of the deposition process onto the manganese crust, we need to estimate the incorporation rate of the radionuclide onto the manganese crust from the ambient water once the radionuclides arrived at the sea floor. The sediment incorporation rate of these radionuclides at the sampling site may be assumed to be equivalent to the fluxes of those

radionuclides arriving at the seafloor, considering their high particle affinity in seawater. The distribution coefficients of these nuclides on a particle are reported to be in the order of  $10^4$ – $10^8$  (You et al., 1989; Geibert and Usbeck, 2004), although the particle dependences of these nuclides are confirmed. The concentrations of  $^{230}\text{Th}$  and  $^{231}\text{Pa}$  in the deep-sea surface sediment in the region of  $5^\circ\text{ N} - 30^\circ\text{ N}$  in latitude and  $147^\circ\text{ E} - 170^\circ\text{ W}$  in longitude were  $1.2$ – $3.2\text{ Bq g}^{-1}$  for  $^{230}\text{Th}$  and  $5.0$ – $6.7 \times 10^{-2}\text{ Bq g}^{-1}$  for  $^{231}\text{Pa}$  (Yang et al., 1986). The  $A_0$  values are calculated to be  $1.3$ – $8.1 \times 10^{-4}\text{ Bq cm}^{-2}\text{ yr}^{-1}$  for  $^{230}\text{Th}$  and  $0.56$ – $1.7 \times 10^{-6}\text{ Bq cm}^{-2}\text{ yr}^{-1}$  for  $^{231}\text{Pa}$  using Eq. (3), assuming that the dried bulk density of the surface deep-sea sediment is  $0.5\text{ g cm}^{-3}$  (Zheng and Yamada, 2005) and that the sedimentation rate is  $2$ – $5\text{ mm kyr}^{-1}$  (Lyle et al., 2005). The deposition rate of  $^{10}\text{Be}$  in the Pacific Ocean was reported to be  $1.0$ – $2.0 \times 10^6\text{ atoms cm}^{-2}\text{ yr}^{-1}$  (Lao et al., 1992). Consequently, the uptake rates onto the manganese crust when compared with the deposition rate onto the deep-sea sediment are estimated to be  $0.11$ – $0.73\%$  for  $^{230}\text{Th}$ ,  $1.4$ – $4.5\%$  for  $^{231}\text{Pa}$ , and  $0.22$ – $0.44\%$  for  $^{10}\text{Be}$ .

On the other hand, a method different from that used for  $^{10}\text{Be}$ ,  $^{230}\text{Th}$ , and  $^{231}\text{Pa}$  is required in order to estimate the uptake rate of  $^{239, 240}\text{Pu}$  because  $^{239, 240}\text{Pu}$  in seawater is not in the steady state in contrast to natural radionuclides. It is considered that the Pu atoms in seawater below  $1551\text{ m}$  the sampling depth of the crust and those in the sediment might have interacted with the manganese crust. From Fig. 5, the inventory of  $^{239, 240}\text{Pu}$  in the manganese crust sampled in 1994 was determined to be  $2.6 \times 10^{-5}\text{ Bq cm}^{-2}$ . The  $^{239, 240}\text{Pu}$  inventory in 1997 below  $1551\text{ m}$  in the seawater column at  $12^\circ\text{ N}$ ,  $165^\circ\text{ E}$  was  $4.6 \times 10^{-3}\text{ Bq cm}^{-2}$  (Livingston et al., 2001) and that in the sediment column at  $11^\circ\text{ N}$ ,  $165^\circ\text{ E}$  was  $1.3 \times 10^{-2}\text{ Bq cm}^{-2}$  (Lee et al., 2005). When compared with its total inventory, the uptake rate of  $^{239, 240}\text{Pu}$  onto the manganese crust is estimated to be  $0.14\%$ , assuming that the  $^{239, 240}\text{Pu}$  distribution did not change significantly between 1994 and 1997.

The deposition rates onto the manganese crust and deep-sea sediment, and the uptake rates of  $^{10}\text{Be}$ ,  $^{230}\text{Th}$ ,  $^{231}\text{Pa}$ , and  $^{239, 240}\text{Pu}$  are summarized in Table 1. The uptake rate of  $^{231}\text{Pa}$

was observed to be ~10 times greater than those of the others. However, the rate corresponding to that of  $^3\text{He}$  was reported to be ~1% by Basu et al. (2006). Helium-3 is known to be a sensitive proxy for guiding extraterrestrial material. It is considered that gaseous  $^3\text{He}$  incorporated into a particle deposits onto the manganese crust; meanwhile,  $^{10}\text{Be}$ ,  $^{230}\text{Th}$ ,  $^{231}\text{Pa}$ , and  $^{239,240}\text{Pu}$  adsorbed onto the surface of a particle also get deposited onto the manganese crust. The re-dissolutions of  $^{10}\text{Be}$ ,  $^{230}\text{Th}$ ,  $^{231}\text{Pa}$ , and  $^{239,240}\text{Pu}$  might occur at the surface of the manganese crust after those nuclides are deposited on the manganese crust together with the sinking particles in contrast to  $^3\text{He}$ . Thus, the uptake rates of  $^{10}\text{Be}$  and  $^{239,240}\text{Pu}$  could be smaller than that of  $^3\text{He}$ . Besides, it is considered that the residence time is correlated with the distribution coefficient on a suspended particle or a sinking particle. It might be the reason why the uptake rates of  $^{10}\text{Be}$  and  $^{239,240}\text{Pu}$  with the long residence times are smaller than the others. On the other hand, it was reported that both the uptake rates of  $^{10}\text{Be}$  and  $^{230}\text{Th}$  onto the manganese crust in the South China Sea were estimated to be ~0.9% (Mangini et al., 1986). These uptake rates estimated by Mangini et al. (1986) correspond roughly to that of  $^{230}\text{Th}$  and  $^{231}\text{Pa}$  estimated in the present work.

It is reported that the deposition rates of  $^3\text{He}$  and  $^{230}\text{Th}$  in such a short duration as a few hundred thousand years are varied (Marcantonio et al., 1996). However, the variation in the deposition rate was not observed to be significant in the present work, because the information resulting from the deposition during a time duration of ~2 Myr was subjected to investigation and information in short durations was averaged. In conclusion, the uptake rate of the sinking particle onto the manganese crust is estimated to be 0.11–4.5% from the results of  $^{10}\text{Be}$ ,  $^{230}\text{Th}$ ,  $^{231}\text{Pa}$  and  $^{239,240}\text{Pu}$ .

### *3.3 Estimation of deposition rate of extraterrestrial material*

A supernova-produced nuclide incorporated into a particle of extraterrestrial material deposits onto the manganese crust as well as  $^3\text{He}$ . Thus, the deposition rate of the

extraterrestrial material could be estimated using the uptake rate of the particle. The influx of the extraterrestrial material all over the earth was estimated to be  $10^4$ – $10^5$  tons  $\text{yr}^{-1}$  (Bernhard and Ravizza, 2000). The  $^{10}\text{Be}$  atoms produced in the upper atmosphere, which are adsorbed onto a particle, migrate in the atmosphere and fall in the ocean; they are finally deposited onto sediments or the manganese crust. It appears that the behavior of extraterrestrial material traveling from the atmosphere to the manganese crust is similar to that of  $^{10}\text{Be}$ . On the basis of the  $^{10}\text{Be}$  concentration data for surface sediments, the deposition rate of  $^{10}\text{Be}$  onto the sediments of the earth's oceans is considered to be roughly homogeneous (Lao et al., 1992; Bourles et al., 1989). Hence, the concentration of extraterrestrial material all over the deep-sea sediment may be homogeneous as well as  $^{10}\text{Be}$ . The deposition rate of extraterrestrial material onto the manganese crust is estimated to be approximately  $2$ – $800 \mu\text{g cm}^{-2} \text{Myr}^{-1}$  according to the surface area of the earth ( $5.1 \times 10^8 \text{ km}^2$ ), influx of extraterrestrial material ( $10^4$ – $10^5$  tons  $\text{yr}^{-1}$ ), and uptake rate of sinking material onto the manganese crust (0.11–4.5%).

On the other hand, the total amount of  $^{10}\text{Be}$  produced in the atmosphere per year is estimated to be  $5.0 \times 10^{24}$  atoms  $\text{yr}^{-1}$  (Nagai et al., 2000). The cosmogenic  $^{10}\text{Be}$  nuclide is oxidized by air immediately after production. Finally, the nuclide adsorbs onto an aerosol including the extraterrestrial material. The residence time of  $\sim 1$  yr for  $^{10}\text{Be}$  in the stratosphere (Raisbeck and Yiou, 1981) corresponds to that of 1–2 yr for aerosol (Capone et al., 1983; Bekki and Pyle, 1994; Jacob, 1997). Thus, the behavior of  $^{10}\text{Be}$  in the atmosphere might be similar to that of the aerosol. If the  $^{10}\text{Be}$  atoms uniformly settle at the sea bottom, a small portion  $8.7 \times 10^{-22}$  from the total production amount of  $^{10}\text{Be}$  atoms is deposited onto a unit area ( $1 \text{ cm}^2$ ) of the manganese crust used for the present work by using the deposition rate onto the manganese crust,  $4.4 \times 10^3$  atoms  $\text{cm}^{-2} \text{yr}^{-1}$  (Table 1). Hence, the deposition rate of extraterrestrial material was estimated to be  $9$ – $90 \mu\text{g cm}^{-2} \text{Myr}^{-1}$ . It should be noted that the concentration dependence of  $^{10}\text{Be}$  and the extraterrestrial material in the upper atmosphere on the latitude are not taken into consideration. In conclusion, the deposition rates of

extraterrestrial material estimated by these two methods are in fair agreement with each other.

The contents of the extraterrestrial material in a unit volume of the manganese crust and deep-sea sediment are estimated to be comparable with each other, although some elements are highly enriched in the manganese crust. The fractionation of elements contained in the extraterrestrial material after depositing onto the manganese crust might be neglected by referring to the depth profile of  $^3\text{He}$  (Basu et al., 2006) for a time scale of  $\sim 10$  Myr. The  $^3\text{He}$  depth profile demonstrates that the degassing of  $^3\text{He}$  is insignificant, i.e., an element incorporated into a particle hardly migrates out of the manganese encrustation. Additionally, the anthropogenic  $^{239,240}\text{Pu}$  contents of the surface of the manganese crust (Lee et al., 2005) were found to be about three orders less than those of the deep-sea sediment.  $^{239,240}\text{Pu}$  atoms were not found in the manganese crust below a depth of 0.5 cm in contrast to the deep-sea sediment in which the  $^{239,240}\text{Pu}$  atoms were detected even at a depth of around 10 cm (Lee et al., 2005; Zheng and Yamada, 2005) from the surface. Hence, the manganese crust may be a better candidate than the deep-sea sediment in searching for the extinct nuclide  $^{244}\text{Pu}$ , which has its origins in outer space.

#### 4. Conclusion

The depth profiles of  $^{10}\text{Be}$ ,  $^{230}\text{Th}$ ,  $^{231}\text{Pa}$ , and  $^{239,240}\text{Pu}$  in the manganese crust were measured in the present work. On the basis of the results of the depth profile of  $^{10}\text{Be}$ , the growth rate of the manganese crust was determined to be  $2.3 \text{ mm Myr}^{-1}$ . When compared with the deposition rates onto the deep-sea sediment, the uptake rates were determined to be 0.22–0.44% for  $^{10}\text{Be}$ , 0.11–0.73% for  $^{230}\text{Th}$ , and 1.4–4.5% for  $^{231}\text{Pa}$  under certain assumptions. When compared with sea water and sediment columns, the uptake rate of  $^{239,240}\text{Pu}$  was determined to be 0.14%. The deposition rate of extraterrestrial material onto the manganese crust was estimated to be  $2\text{--}800 \mu\text{g cm}^{-2} \text{ Myr}^{-1}$  by using the abovementioned

uptake rates. Additionally, the deposition rate was estimated to be 9–90  $\mu\text{g cm}^{-2} \text{Myr}^{-1}$  by using the production rate of  $^{10}\text{Be}$  on the entire earth and the deposition rate of  $^{10}\text{Be}$  onto the manganese crust. The deposition rates of extraterrestrial material estimated by these two methods are in fair agreement with each other.

## Acknowledgements

We would like to thank the members of the Japan Oil, Gas and Metals National Corporation for their assistance in sampling and supplying the manganese crust. We also wish to acknowledge the assistance of the members of the Research Center for Nuclear Science and Technology, University of Tokyo, with regard to the accelerator mass spectrometry of  $^{10}\text{Be}$ . The author is deeply indebted to Professor Y. Sano of University of Tokyo, and an anonymous reviewer who have given their valuable comments to improve the manuscript.

## References

- Aarkrog, A. (2003): Input of anthropogenic radionuclides into the world ocean. *Deep-Sea Res.* **II 50**, 2597–2606.
- Basu, S., F. M. Stuart, V. Klemm, G. Korschinek, K. Knie, J. R. Hein (2006): Helium isotopes in ferromanganese crust from the central Pacific Ocean. *Geochim. Cosmochim. Acta* **70**, 3996–4006.
- Bekki, S., J. A. Pyle (1994): A two-dimensional modeling study of the volcanic eruption of Mount Pinatubo. *J. Geophys. Res. D.* **99**, 18,861–18,870.
- Bernhard, P. E. and G. Ravizza (2000): The effects of sampling artifacts on cosmic dust flux estimates: A reevaluation of nonvolatile tracers (Os, Ir). *Geochim. Cosmochim. Acta* **64**, 1965–1970.

- Bourles, D., G. M. Raisbeck and F. Yiou (1989):  $^{10}\text{Be}$  and  $^9\text{Be}$  in marine sediments and their potential for dating. *Geochim. Cosmochim. Acta* **53**, 443–452.
- Buesseler, K. O. (1997): The isotopic signature of fallout plutonium in the North Pacific. *J. Environ. Radioactivity* **36**, 69–83.
- Capone, L. A., W. B. Toon, R. C. Whitten, R. P. Turco, C. A. Riegel (1983): A two-dimensional model simulations of the El Chichon volcanic eruption cloud. *Geophys. Res. Lett.* **10**, 1053–1056.
- Geibert, W. and R. Usbeck (2004): Adsorption of thorium and protactinium onto different particle type: Experimental findings. *Geochim. Cosmochim. Acta* **68**, 1489–1501.
- Jacob, D. J. (1997): *Introduction to atmospheric chemistry*. Princeton. University Press. pp. 70.
- Knie, K., G. Korschinek, T. Faestermann, C. Wallner, J. Scholten and W. Hillebrandt (1999): Indication for supernova produced  $^{60}\text{Fe}$  activity on earth. *Phys. Rev. Lett.* **83**, 18–21.
- Knie, K., G. Korschinek, T. Faestermann, E. A. Dorfi, G. Rugel and A. Wallner (2004):  $^{60}\text{Fe}$  anomaly in a deep-sea manganese crust and implications for a nearby supernova source. *Phys. Rev. Lett.* **93**, 171103.
- Lao, Y., R. F. Anderson, W. S. Broecker, S. E. Trumbore, H. J. Hofmann and W. Wolfli (1992): Transport and burial rates of  $^{10}\text{Be}$  and  $^{231}\text{Pa}$  in the Pacific Ocean during the Holocene period. *Earth Planet. Sci. Lett.* **113**, 173–189.
- Lao, Y., R. F. Anderson, W. S. Broecker, H. J. Hofmann and W. Wolfli (1993): Particulate fluxes of  $^{230}\text{Th}$ ,  $^{231}\text{Pa}$ , and  $^{10}\text{Be}$  in the northeastern Pacific Ocean. *Geochim. Cosmochim. Acta* **57**, 205–217.
- Lee, S., P. P. Povinec, E. Wyse, M. K. Pham, G. Hong, C. Chung, S. Kim and H. Lee (2005): Distribution and inventories of  $^{90}\text{Sr}$ ,  $^{137}\text{Cs}$ ,  $^{241}\text{Am}$ , and Pu isotopes in sediments of the Northwest Pacific Ocean. *Mar. Geol.* **216**, 249–263.
- Livingston, H. D. and R. F. Anderson (1983): Large particle transport of plutonium and other

- fallout radionuclides to the deep ocean. *Nature* **303**, 228–231.
- Livingston, H. D., P. P. Povinec, T. Ito and O. Togawa (2001): The behaviour of plutonium in the Pacific Ocean. In *Plutonium in the Environment* (ed. Kudo A.). Elsevier Science, Amsterdam, pp. 267–292.
- Lyle, M., N. Mitchell, N. Pisiias, A. Mix, J. I. Martinez and A. Paytan (2005): Do geochemical estimates of sediment focusing pass the sediment test in the equatorial Pacific? *Paleoceanography* **20**, PA1005.
- Mangini, A., M. Segl, H. Kudrass, M. Wiedicke, G. Bonani, H. J. Hofmann, E. Morenzoni, M. Nessi, M. Suter and W. Wöfli (1986): Diffusion and supply rates of  $^{10}\text{Be}$  and  $^{230}\text{Th}$  radioisotopes in two manganese encrustations from the South China Sea. *Geochim. Cosmochim. Acta* **50**, 149–156.
- Marcantonio, F., R. F. Anderson, M. Stute, N. Kumar, P. Schlosser and A. Mix (1996): Extraterrestrial  $^3\text{He}$  as a tracer of marine sediment transport and accumulation. *Nature* **383**, 705–707.
- Matsuzaki, H., M. Tanikawa, K. Kobayashi and S. Hatori (2000): Development of a gas counter for AMS measurement of  $^{10}\text{Be}$  and  $^{26}\text{Al}$  of cosmic spherules. *Nucl. Instrum. Meth.* **B172**, 218–223.
- Nagai, H., W. Tada and T. Kobayashi (2000): Production rates of  $^7\text{Be}$  and  $^{10}\text{Be}$  in the atmosphere. *Nucl. Instrum. Meth.* **B172**, 796–801.
- Raisbeck, G. M. and F. Yiou (1981): Cosmogenic  $^{10}\text{Be}/^7\text{Be}$  as a probe of atmospheric transport processes. *Geophys. Res. Lett.* **8**, 1015–1018.
- Sano, Y., K. Toyoda and H. Wakita (1985):  $^3\text{He}/^4\text{He}$  ratios of marine ferromanganese nodules. *Nature* **317**, 518–520.
- Schultz, M. K., M. Hammond, J. T. Cessna, P. Plascjak, B. Norman, L. Szajek, K. Garmestani, B. E. Zimmerman and M. Unterweger (2006): Assessing the  $^{210}\text{At}$  impurity in the production of  $^{211}\text{At}$  for radiotherapy by  $^{210}\text{Po}$  analysis via isotope dilution alpha

- spectrometry. *Appl. Radiat. Isot.* **64**, 1365–1369.
- Shibata, S., M. Imamura, K. Sakamoto, S. Okizaki, S. Shibutani, H. Matsumura, M. Furukawa, I. Fujiwara, H. Nagai and K. Kobayashi (1998): Yield measurement of  $^7\text{Be}$  and  $^{10}\text{Be}$  produced by photonuclear reactions at intermediate energies: intercomparison of fragmentation processes between photon- and proton-induced reactions. *Radiochim Acta* **80**, 181–187.
- UNSCEAR (2000): Sources and effects of ionizing radiation, United Nations Scientific Committee on the Effects of Atomic Radiation, United Nations, New York.
- Wallner, C., T. Faestermann, U. Gerstmann, W. Hillebrandt, K. Knie, G. Korschinek, C. Lierse, C. Pomar and G. Rugel (2000): Development of a very sensitive AMS method for the detection of supernova-produced longliving actinide nuclei in terrestrial archives. *Nucl. Instrum. Meth.* **B172**, 333–337.
- Wallner, C., T. Faestermann, U. Gerstmann, K. Knie, G. Korschinek, C. Lierse and G. Rugel (2004): Supernova produced and anthropogenic  $^{244}\text{Pu}$  in deep-sea manganese encrustations. *New Astro. Rev.* **48**, 145–150.
- Yang, H., Y. Nozaki and H. Sakai (1986): The distribution of  $^{230}\text{Th}$  and  $^{231}\text{Pa}$  in the deep-sea surface sediments of the Pacific Ocean. *Geochim. Cosmochim. Acta* **50**, 81–89.
- You, C. F., T. Lee and Y. H. Li (1989): The partition of Be between soil and water. *Chem. Geol.* **77**, 105–118.
- Zheng, J. and M. Yamada (2005): Vertical distributions of  $^{239+240}\text{Pu}$  activities and  $^{240}\text{Pu}/^{239}\text{Pu}$  atom ratios in sediment cores: implications for the sources of Pu in the Japan Sea. *Sci. Tot. Environ.* **340**, 199–211.

Table 1

Uptake rates of  $^{239, 240}\text{Pu}$ ,  $^{230}\text{Th}$ ,  $^{231}\text{Pa}$  and  $^{10}\text{Be}$  onto the manganese crust, deposition rates of  $^{230}\text{Th}$ ,  $^{231}\text{Pa}$  and  $^{10}\text{Be}$  onto the crust and deep-sea sediment, inventory of  $^{239, 240}\text{Pu}$  in the crust, and that of  $^{239, 240}\text{Pu}$  in seawater below 1551 m and sediment column near sampling station.

Nuclide	Deposition rate onto manganese crust	Calculated deposition rate onto deep-sea sediment	Uptake rate
Th-230	$9.2 \times 10^{-7} \text{ Bq cm}^{-2} \text{ yr}^{-1}$	$1.3\text{--}8.1 \times 10^{-4} \text{ Bq cm}^{-2} \text{ yr}^{-1}$	0.11–0.73%
Pa-231	$2.5 \times 10^{-7} \text{ Bq cm}^{-2} \text{ yr}^{-1}$	$0.56\text{--}1.7 \times 10^{-6} \text{ Bq cm}^{-2} \text{ yr}^{-1}$	1.4–4.5%
Be-10	$4.4 \times 10^3 \text{ atoms cm}^{-2} \text{ yr}^{-1}$	$1.0\text{--}2.0 \times 10^6 \text{ atoms cm}^{-2} \text{ yr}^{-1}$	0.22–0.44%
Nuclide	Inventory in manganese crust	Inventory in seawater and sediment column	Uptake rate
Pu-239, 240	$2.6 \times 10^{-5} \text{ Bq cm}^{-2}$	$1.8 \times 10^{-2} \text{ Bq cm}^{-2}$	0.14%

## Figure Captions

Fig. 1.

Alpha spectra of Pu isotopes measured for 16 days for the manganese crust in the 0–0.5-cm section (a) and for 10 days in 0.5–1.0-cm section (b). Expanded spectrum of the  $^{239,240}\text{Pu}$  peak region is also shown.

Fig. 2.

Depth profile of the  $^{10}\text{Be}$  atoms. Propagated  $1\sigma$  of the statistical error is shown.

Fig. 3.

Depth profile of the  $^{230}\text{Th}$  activity (a) and  $^{230}\text{Th}/^{238}\text{U}$  activity ratio (b). Propagated  $1\sigma$  of the statistical error is shown in (a); the  $1\sigma$  of the statistical error for the measurement of Th isotope and standard deviation obtained by performing the measurements of U concentration five times by an ICP-MS are propagated is shown in (b).

Fig. 4.

Depth profile of the  $^{231}\text{Pa}$  activity (a) and  $^{231}\text{Pa}/^{235}\text{U}$  activity ratio (b). Each of errors was derived by the same manner described in the caption of figure 3.

Fig. 5.

Depth profile of the  $^{239,240}\text{Pu}$  activity. Propagated  $1\sigma$  of the statistical error and detection limit (broken line) are shown.

Fig. 6.

Depth profile of  $^{238}\text{U}$  activity.  $1\sigma$  of the standard deviation obtained by performing the

ICP-MS measurements five times are shown.

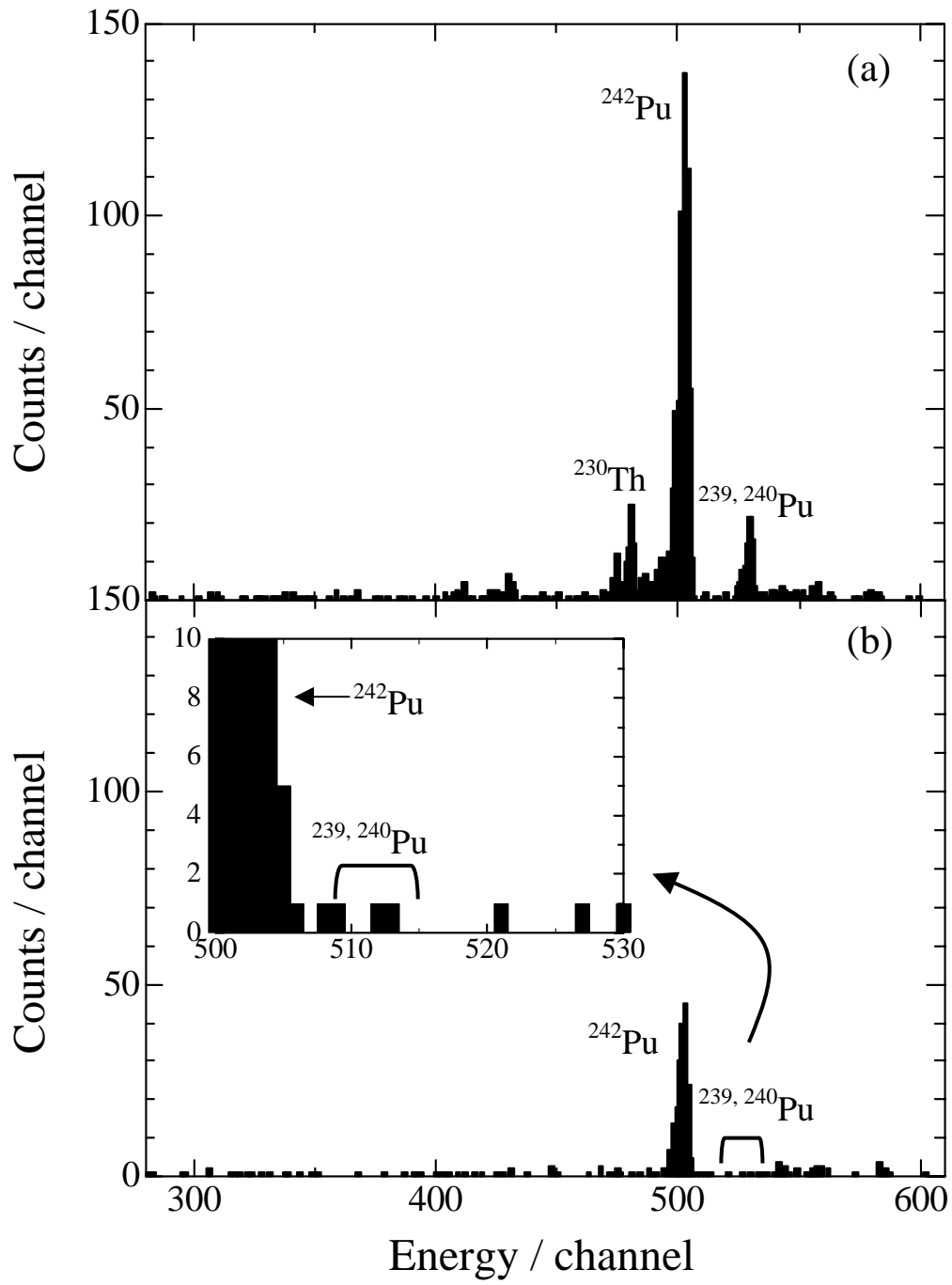


Figure 1

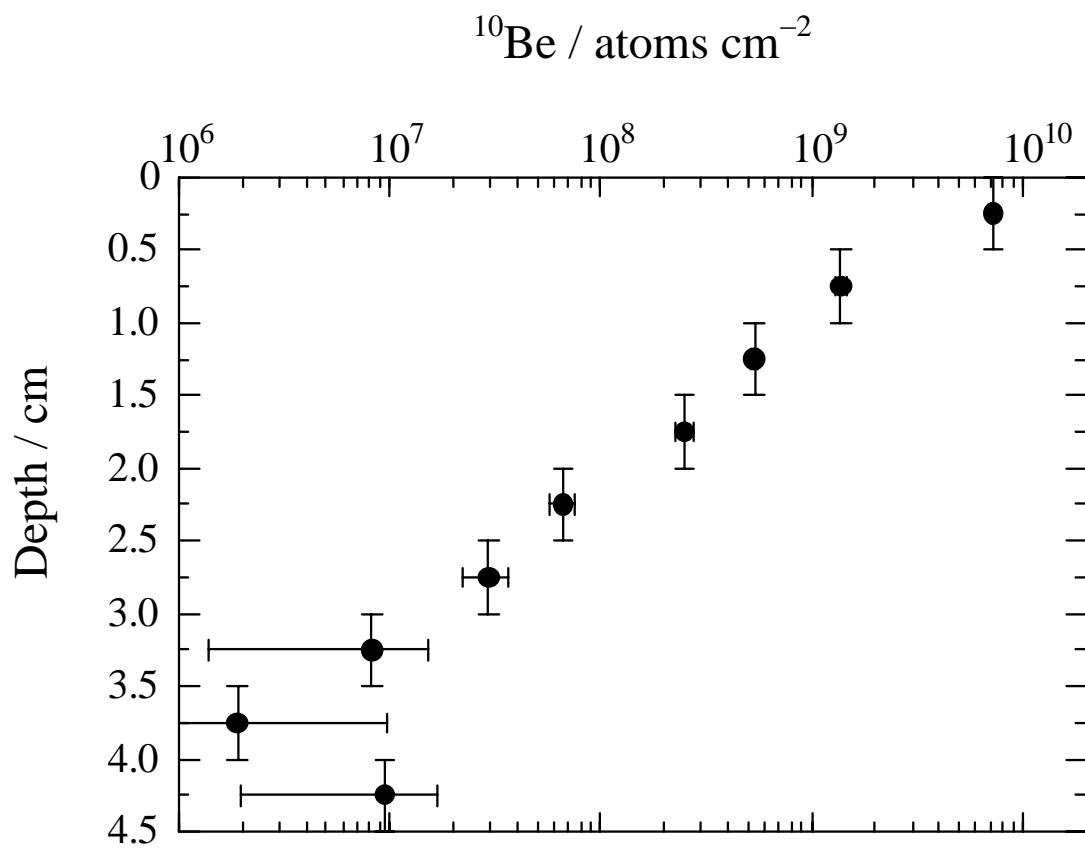


Figure 2

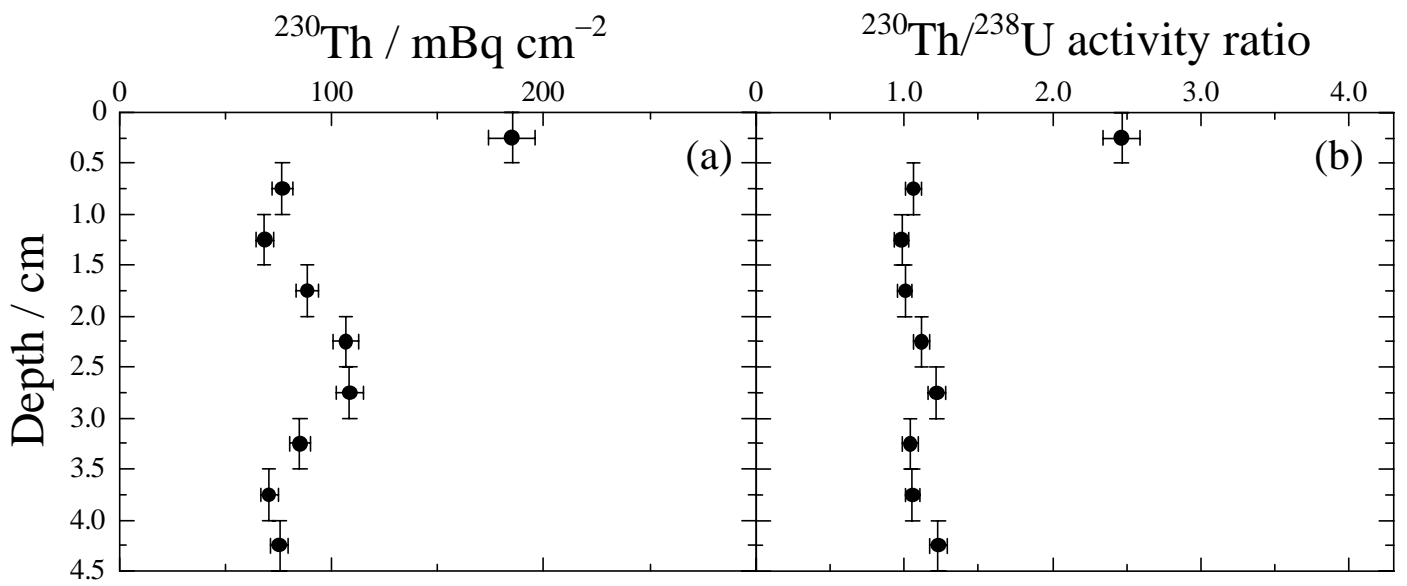


Figure 3

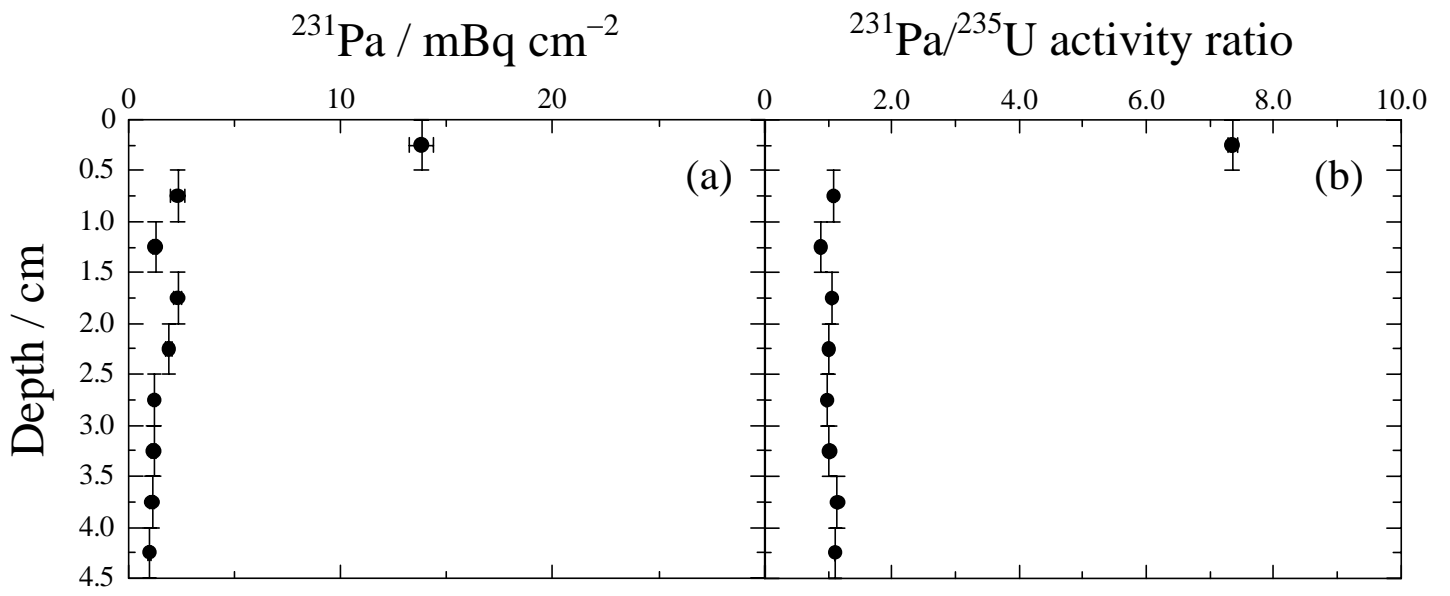


Figure 4

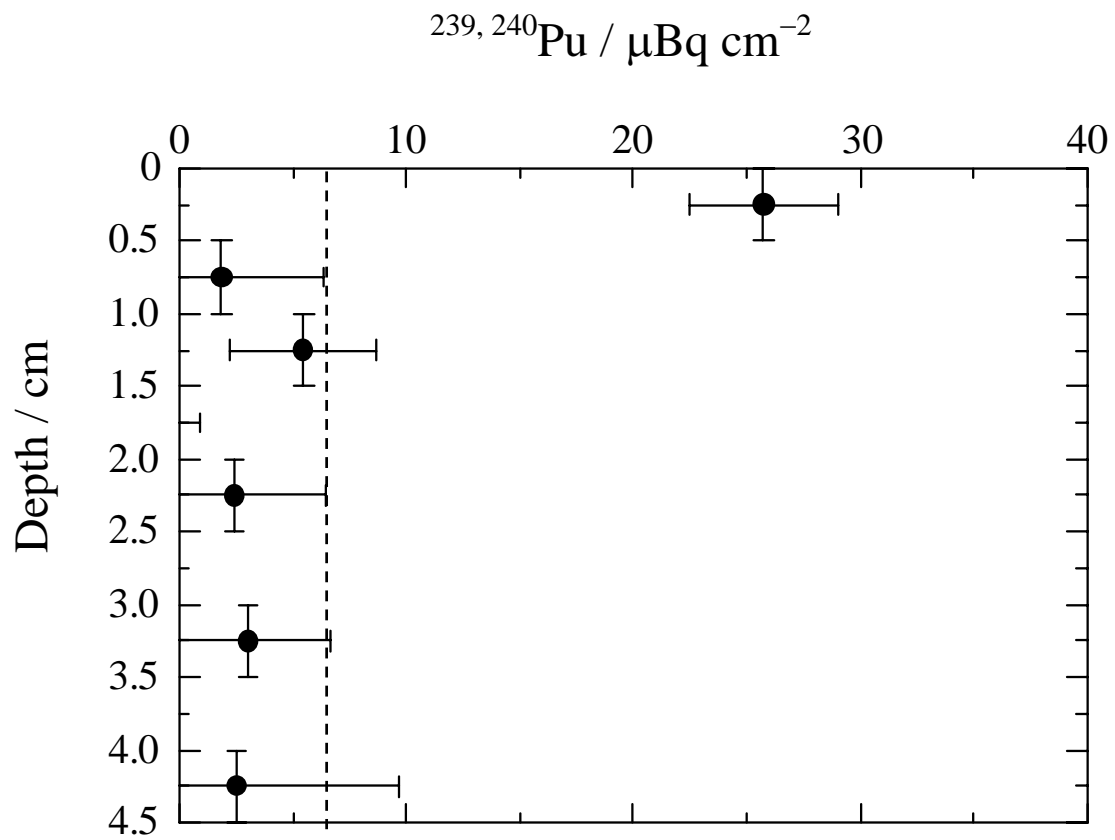


Figure 5

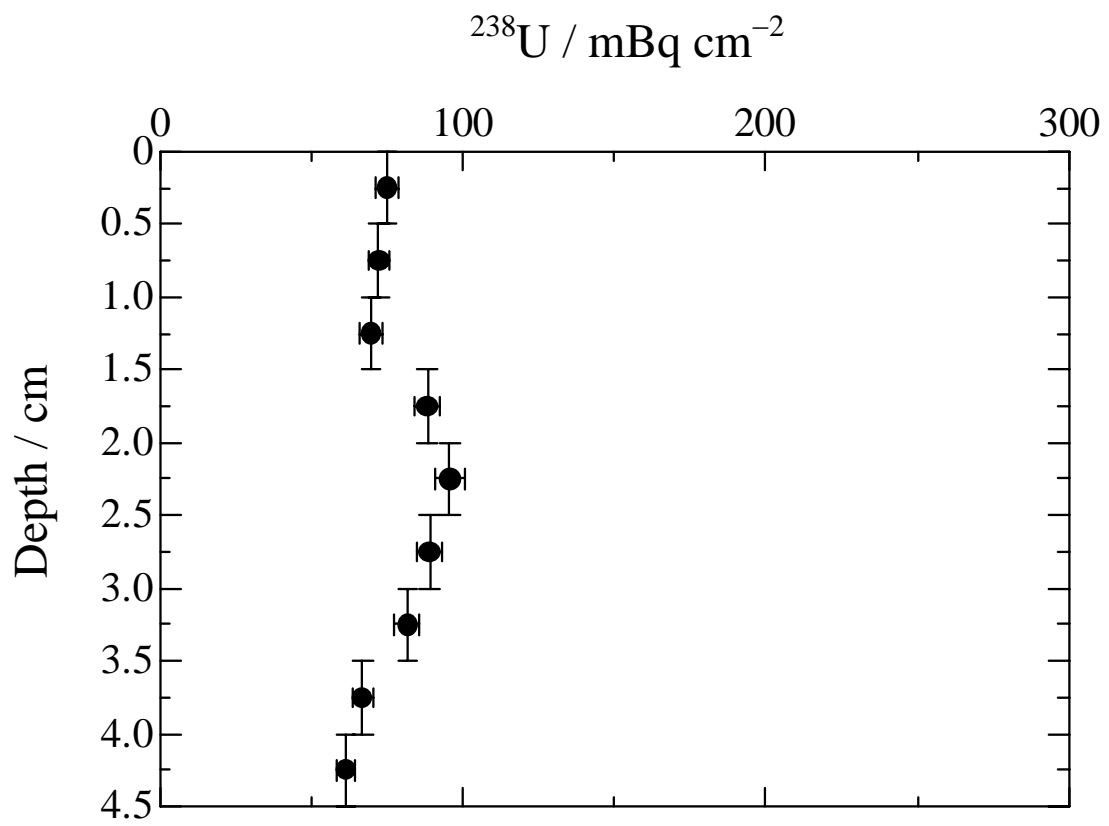


Figure 6